Tonehole Radiation Directivity: A Comparison Of Theory To Measurements

Gary P. Scavone[1] Matti Karjalainen[2]
gary@ccrma.stanford.edu Matti.Karjalainen@hut.fi

[1]Center for Computer Research in Music and Acoustics
Department of Music, Stanford University
Stanford, California 94305-8180 USA

[2]Laboratory of Acoustics and Audio Signal Processing
Helsinki University of Technology
FIN-02015 HUT, Espoo, Finland

Abstract

Measurements have been conducted in an anechoic chamber for comparison to current linear acoustic theory for radiation directivity from a cylindrical pipe with toneholes. Time-delay spectrometry using an exponentially swept sine signal was employed to determine impulse responses at points external to the experimental air column. This technique is effective in clearly isolating nonlinear artifacts from the desired linear system response along the time axis, allowing the use of a strong driving signal without fear of nonlinear distortion. The experimental air column was positioned through a wall conduit into the anechoic chamber such that the driver and pipe input were located outside the chamber while the open pipe end and toneholes were inside the chamber, effectively isolating the source from the pickup. Measured results are compared to both frequency-domain, transmission-network simulations, as well as time-domain, digital waveguide calculations.

1 Introduction

A variety of wind instrument tonehole models have been developed and implemented using both frequency- and time-domain methods [Keefe 1990, Välimäki et al. 1993, Scavone and Smith 1997, van Walstijn and Scavone 2000]. These studies were primarily concerned with the *internal* scattering characteristics of toneholes in an air column model. Rousseau [1996] reported comparisons of a frequency-domain tonehole radiation model to a discrete set of two-dimensional polar frequency-domain measurements. A discrete-time implementation of this tonehole radiation model was discussed by Scavone [1999]. The present paper compares both time- and frequency-domain tonehole radiation model results to a set of measurements conducted in an anechoic chamber using time-spectrometry techniques.

2 Tonehole Acoustic Theory

Keefe [1982] presented the first detailed study of linear tonehole acoustic theory. Using frequency-domain, transmission-network methods, the tonehole junction is represented by a two-port element as shown in Fig. 1. The shunt impedance component, Z_s, characterizes the properties of the tonehole branch, while the series impedances (Z_a) represent negative length corrections to the main air column due to the presence of the tonehole.

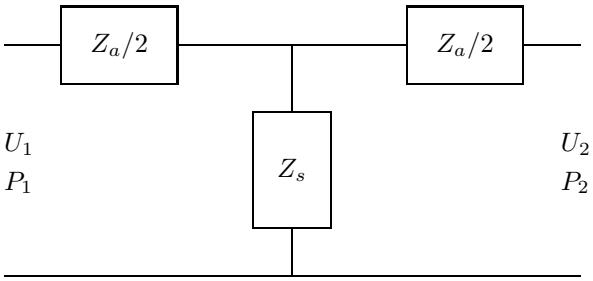

Figure 1: T section transmission-line element representing the tonehole.

Two-port digital waveguide implementations of Keefe's representation were discussed in Scavone and Smith [1997] and Smith and Scavone [1997]. While the discrete-time implementation produced excellent agreement with Keefe's results, the model was limited in its ability to allow tonehole state changes. Subsequent models to implement a dy-

namic tonehole state were reported by Scavone and Cook [1998] and van Walstijn and Scavone [2000]. In general, excellent agreement between the frequency- and time-domain results for *internal* wave propagation has been achieved, even when low-frequency approximations are used to simplify the implementations.

Rousseau [1996] incorporated the results of Levine and Schwinger [1948] to model tonehole radiation and directivity from an unflanged cylindrical pipe. Figure 2 shows the radiation directivity calculated for a pipe of 2 centimeter radius.

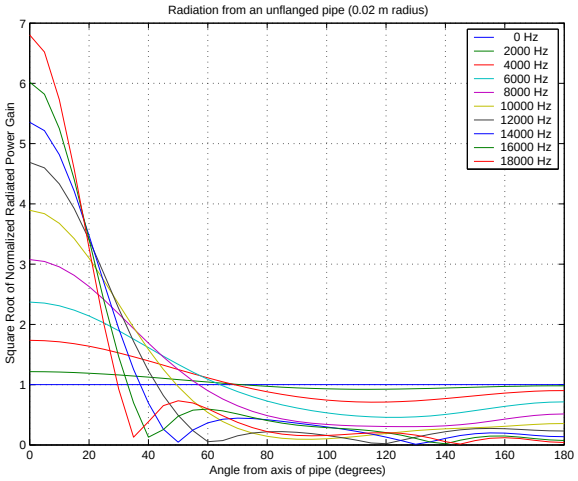

Figure 2: Radiation directivity vs. angle from pipe end.

Toneholes are typically partly flanged and partly unflanged, so that an intermediate model between these two cases would be most appropriate. However, an appropriate analytic solution for real tonehole geometries would be a non-trivial endeavor.

This study makes exclusive use of the Levine and Schwinger model. Directivity filters are designed for specific tonehole-to-pickup angles, as reported in [Scavone 1999]. Wave propagation in free space is based on a lossless, near-field model, though the standard $1/r$ pressure dependence is incorporated in the models.

3 Data Acquisition

The directivity measurements for this study were conducted in an anechoic chamber at the Laboratory of Acoustics and Audio Signal Processing, Helsinki University of Technology using an experimental setup consisting of an aluminum cylindrical pipe of five meters length, 0.021 meter inner diameter, and 0.025 meter outer diameter. Two toneholes, each of 0.009 meter diameter, were drilled 0.1575 and 0.0945 meters from the output end of the pipe. The pipe was inserted through a duct in the chamber wall such that its input end was located outside the chamber and the output end was located inside the chamber, effectively isolating the driver and external microphones from one another. A Beyerdynamic DT880 headphone speaker was attached to the input of the pipe and driven directly from the output of a Power Macintosh computer soundcard. QuickSig DSP and measurement software was used for the signal generation and data acquisition, including source signal deconvolution [Karjalainen 1990].

The measurement setup presented significant problems because of low signal radiation from inside the cylindrical pipe to the external microphone. Measurement contamination due to nonlinear driver distortion was an additional concern. The use of an anechoic chamber minimized the ambient noise level, but a reasonable signal-to-noise ratio necessitated a powerful source signal. Despite having desirable source strength characteristics, maximum length sequence techniques were rejected because of weaknesses in the presence of system non-linearities.

With these conditions in mind, a log-swept chirp signal of the form

$$x(t) = \sin\left[\frac{\omega_1 T}{\ln\left(\frac{\omega_2}{\omega_1}\right)}\left(e^{\frac{t}{T}\ln\left(\frac{\omega_2}{\omega_1}\right)} - 1\right)\right]$$

was chosen for this experiment [Farina 2000]. Chirp techniques are advantageous when nonlinear distortion may be present in a measurement system because linear and non-linear responses are clearly isolated in the time domain result via linear deconvolution. In addition, the log-swept chirp provides a better measure of a system's low-frequency response, where measurement difficulties are typical, because of greater low-frequency signal energy.

The microphone positions used during the measurements are illustrated in Fig. 3. All measurements were made using the same microphone (1/8 inch, Sennheiser KE4-211-2) and preamp (Unides Design). Two internal measurements were taken at the pipe input (0.0655 meters) and near the pipe center (2.0015 meters). External measurements were taken at a fixed radius (0.1285 meters) from the hole lattice center at 30 degree intervals within a plane bisecting the toneholes and pipe end, as illustrated in Fig. 4. Measurements were made for

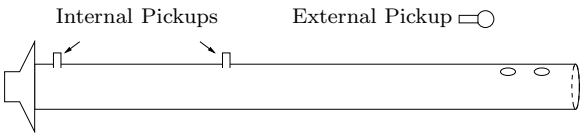

Figure 3: Internal and external pickup locations.

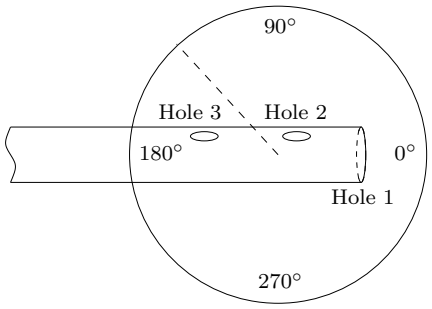

Figure 4: Fixed radius external measurement plane.

four different fingerings, varying both the tonehole and pipe end states. The computer sampling rate was 44100 Hz.

4 Data Processing

Results were obtained by deconvolution (division in the frequency domain) of the recorded external response by the log-swept source signal [Karjalainen et al. 1995]. An internal measurement, shown in Fig. 5, was made near the pipe input to capture the combined responses of the computer soundcard, headphone driver, and microphone system. This measurement system response was then deconvolved from the external results. While difficult to discern in Fig. 5, the measurement system produced reliable low-frequency results down to about 150 Hz.

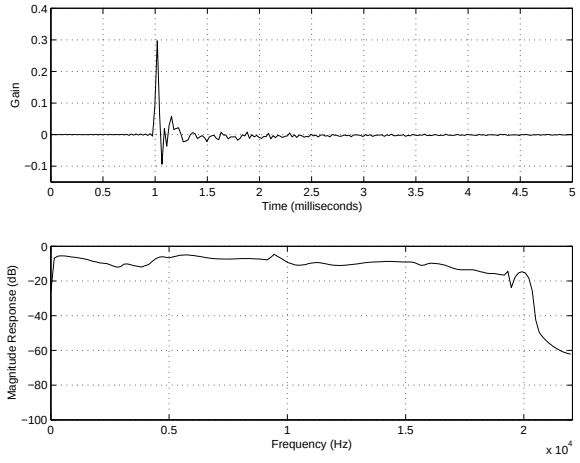

Figure 5: Measured internal response near pipe input.

The second internal pipe response measurement was made to allow the calculation and possible compensation of viscothermal losses occurring for internal wave propagation from the pipe input to the first tonehole. This measurement was not used in the results reported here because viscothermal losses were already incorporated in the models.

5 Measurements vs. Models

The processed measurements represent the radiated impulse responses of the experimental system recorded externally at different pickup points. In the following plots, these responses are compared with the results obtained using a discrete-time, digital waveguide model and a frequency-domain, transmission-network model of the same system. The measured data shows a consistent "notch" above 9 kHz, which is consistent with the first cross-mode for a pipe of this radius. Because the *models* are based on propagation in just one-dimension, the frequency-domain plots are limited to a range of 10 kHz.

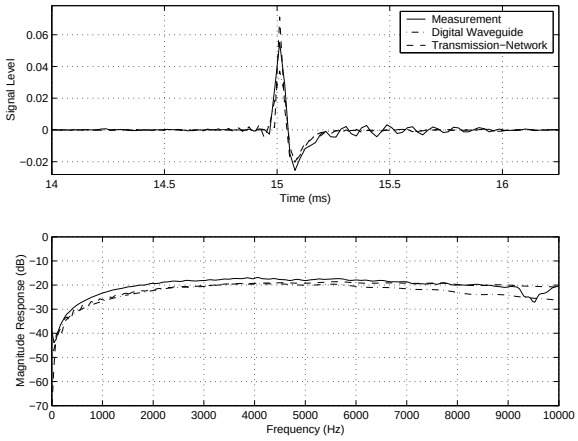

Figure 6: Open holes: 1; Closed holes: 2 & 3. Measurement angle: 210°.

In general, there is good "first-order" agreement between the measurements and models, both in terms of temporal features and frequency magnitude contours. For example, the response of the system with all holes open is shown in Fig 8. In the top plot, the pickup is located directly above the toneholes. The pickup is located directly "behind" the toneholes in the bottom plot. In the time domain response, the radiated impulse components from the toneholes are first recorded, followed by radiation from the open end of the pipe.

A few consistent discrepancies can be observed. In particular, "rear angle" radiation appears to be overestimated using the Levine and Schwinger model (compare the top and bottom plots of Fig. 7–9). This can be partly attributed to the use of the *unflanged* tonehole model. Relative phase differences between tonehole and open-end "events" can be partially explained by the fact that the models implement a one-dimensional system.

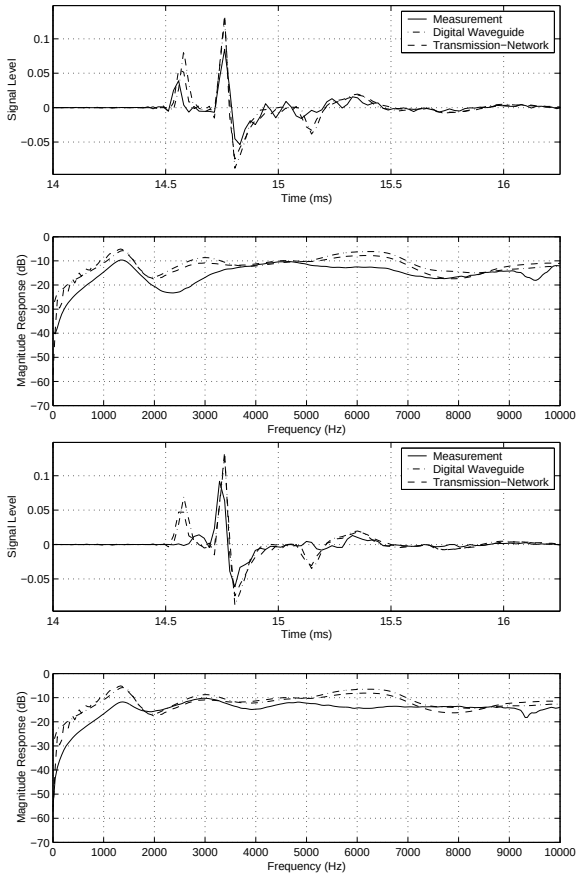

Figure 7: Open holes: 1 & 2; Closed holes: 3. Measurement angles: 60° (top), and 300° (bottom).

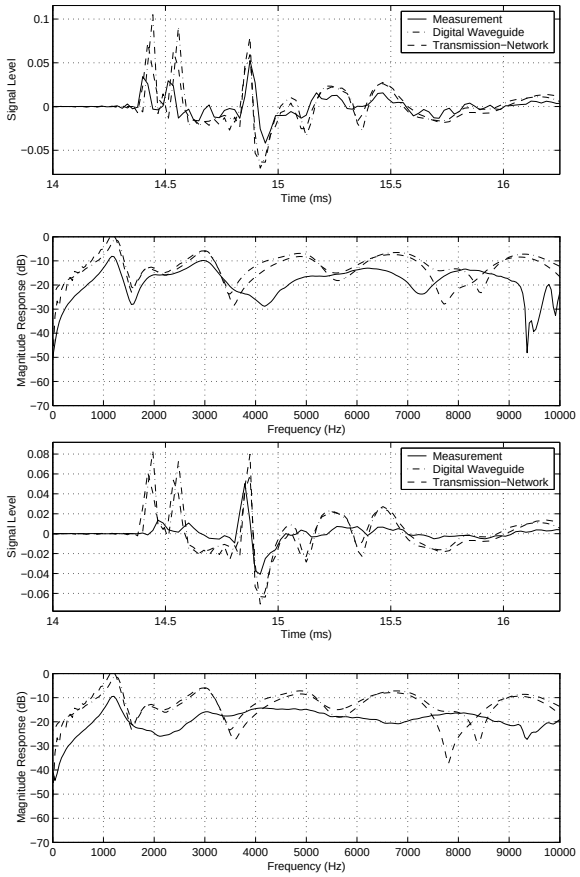

Figure 8: All holes open. Measurement angles: 90° (top) and 270° (bottom).

That is, the toneholes are represented by point-sources located at their midpoint along the principal axis of the pipe. Depending on the pickup location, the models will overestimate the propagation delay by an amount corresponding to half the hole diameter. In addition, when the pickup is located "below" a tonehole (angles between 210° and 330°), propagation delay across half the pipe diameter is neglected (as well as delay attributable to the pipe curvature). These affects are visible in Figs. 7 and 8.

Closed-hole reflections are evident in the model results but more difficult to discern in the measurements (see Fig. 6).

6 Summary

The measurement technique applied in this study appears to provide good results over a wide frequency range, with particular improvement at low frequencies.

The measurements and model results show good "first-order" temporal and spectral agreement. Some discrepancies are apparent, most of which can be explained in terms of model simplifications. It appears that the unflanged open-hole model over-estimates rear-angle directivity.

References

A. Farina. Simultaneous measurement of impulse response and distortion with a swept-sine technique. *Audio Engineering Society*, Feb. 2000. Presented at the 108th AES Convention, Paris, France.

M. Karjalainen. DSP software integration by object-oriented programming: a case study of QuickSig. *IEEE ASSP Magazine*, pages 21–31, Apr. 1990.

M. Karjalainen, J. Huopaniemi, V. Välimäki, and B. Hernoux. Explorations of wind instruments using digital signal processing and physical modeling techniques. *Journal of New Music Research*, 24(4):301–317, 1995.

D. H. Keefe. Theory of the single woodwind tone hole. *J. Acoust. Soc. Am.*, 72(3):676–687, Sept. 1982.

D. H. Keefe. Woodwind air column models. *J. Acoust. Soc. Am.*, 88(1):35–51, July 1990.

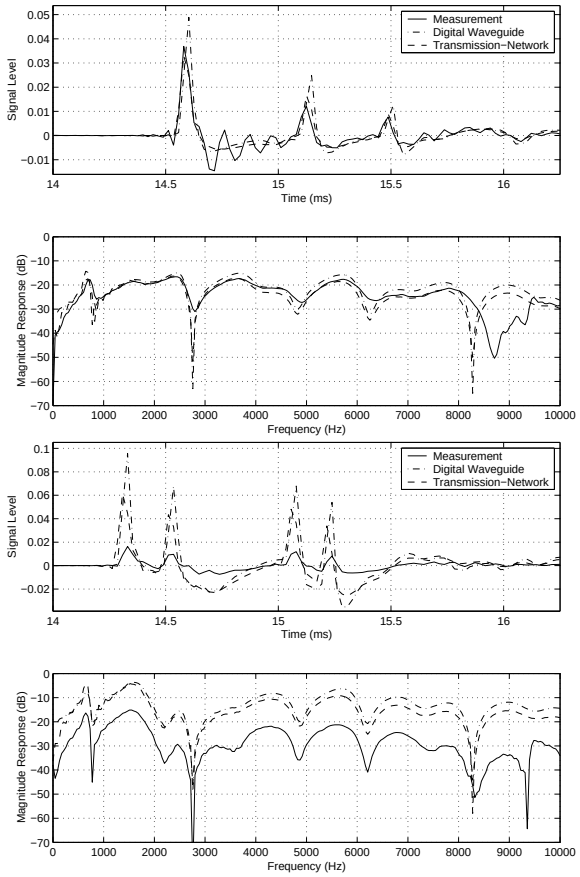

Figure 9: Open holes: 2 & 3; Closed holes: 1. Measurement angles: 0° (top) and 240° (bottom).

H. Levine and J. Schwinger. On the radiation of sound from an unflanged circular pipe. *Phys. Rev.*, 73(4):383–406, Feb. 1948.

A. Rousseau. Modélisation du rayonnement des instruments à vent à trous latéraux. Technical report, Institut de Recherche et Coordination Acoustique/Musique, Département d'acoustique instrumentale (responsable: René Caussé), May 1996.

G. P. Scavone. Modeling wind instrument sound radiation using digital waveguides. In *Proc. 1999 Int. Computer Music Conf.*, pages 355–358, Beijing, China, 1999. Comp. Music Assoc.

G. P. Scavone and P. R. Cook. Real-time computer modeling of woodwind instruments. In *Proc. Int. Symp. on Musical Acoustics (ISMA-98), Leavenworth, WA*, pages 197–202, June 1998.

G. P. Scavone and J. O. Smith. Digital waveguide modeling of woodwind toneholes. In *Proc. 1997 Int. Computer Music Conf.*, pages 260–263, Thessaloniki, Greece, 1997. Comp. Music Assoc.

J. O. Smith and G. P. Scavone. The one-filter Keefe clarinet tonehole. In *Proc. IEEE Workshop on Applied Signal Processing to Audio and Acoustics*, pages 19–22, New York, Oct. 1997. IEEE Press.

V. Välimäki, M. Karjalainen, and T. I. Laakso. Modeling of woodwind bores with finger holes. In *Proc. 1993 Int. Computer Music Conf.*, pages 32–39, Tokyo, Japan, 1993. Comp. Music Assoc.

M. van Walstijn and G. P. Scavone. The wave digital tonehole model. In *Proc. 2000 Int. Computer Music Conf.*, pages 465–468, Berlin, Germany, 2000. Comp. Music Assoc.